

## Designing Plane Wave Modulators Using 1DPC Nanostructure with r-GRIN Defect Layer

Kazem Jamshidi-Ghaleh<sup>1, 2</sup> and Farzaneh Bayat<sup>1, \*</sup>

**Abstract**—In this paper, we introduce plane wave modulators that are designed using one-dimensional photonic crystals (1DPC) containing radial gradient refractive index (r-GRIN) defect layers. Three kinds of r-GRIN materials with different refractive index distribution functions are applied in numerical analysis. The properties of the phase and intensity of the transmitted plane wave beam through proposed structures are studied using the transfer matrix method. Radially-dependent defect modes, modulated phase and intensity are obtained according to the refractive index distribution functions. The results are predictable by regarding the Bragg condition and destructive interference, which are the origins of the photonic band gap (PBG). Due to the radial-dependency of the defect layer's refractive index, the rays passing through different transverse positions experience different optical pathways. Therefore, the defect modes and transmitted spectrum (phase and amplitude) vary transversely. This study demonstrates another ability of the artificial PC structures to design plane wave modulators and manipulate its phase and intensity.

### 1. INTRODUCTION

Over a century ago, in 1885, Rayleigh [1], for the first time, investigated purely periodic system extending to infinity in one direction. He found out that in these structures there are special wavelengths ranges that electromagnetic waves with these wavelengths are forbidden to propagate inside them. Nowadays this periodic arrangement of layers, having different materials in its layers, is called 1DPC, introduced first time by Yablonovitch [2] and John [3]. They are designed to control and manipulate the propagation of light [4–9]. It is called a crystal, because of its periodicity, and photonic because it acts on light. A PC can be made with refractive index modulation of a medium either by arranging a lattice of air holes in the materials or by forming a lattice of high refractive index material embedded in a transparent medium with a lower refractive index in one, two or three dimensions. Different arrangements of 1DPC structures have attracted much attention because it can be easily fabricated by modern experimental techniques. The main characteristic of a PC structure is the PBG; the range of wavelengths of the incident light that cannot propagate through the structure. If the periodicity of PC structure is broken by introducing a different layer in nature (materials and size) or disordering the layers, it is possible to create highly localized defect modes within the PBG [10–12]. The origin of the PBG in the transmitted wave, in 1DPC structures, results from the destructive interference among the waves scattered by interfaces of the layers in the forward direction. In the normal incident case, the characteristics of the PBGs and defect modes, closely depend on the optical properties of the constituted layers and defect layer. The existence of the PBG and defect modes in the optical spectrum (Reflectance, Absorptance or Transmittance) of the PC have led to many interesting phenomena and numerous applications of PCs in improving the performance of optoelectronic and microwave devices such as high-efficiency semiconductor lasers, light emitting diodes, wave guides, high-Q resonators, antennas, all-optical diodes and filters, frequency selective surface, optical limiters and amplifiers [13–16].

---

*Received 30 October 2013, Accepted 6 December 2013, Scheduled 9 December 2013*

\* Corresponding author: Farzaneh Bayat (f.bayat@azaruniv.edu).

<sup>1</sup> Department of Physics, Azarbaijan Shahid Madani University, Tabriz, Iran. <sup>2</sup> Research Group of Processing and Communication, Azarbaijan Shahid Madani University, Tabriz, Iran.

In most of the previous works, a conventional 1DPC structure with different arrangements of materials under irradiation of the plane wave (the phase and amplitude are constant in the transverse direction) are studied that the refractive indexes of the layers are considered to be constant in the lateral direction (perpendicular to the periodicity of the structure). In refs [17, 18] we have obtained the transfer matrix and studied the transmittance spectrum of 1DPC structure under irradiation of the Gaussian beam (the phase and amplitude are varying laterally). Recently, a binary 1DPC structure has been proposed that the refractive index of layers A and B is a function of space position [19, 20]. They have presented the effects of the incident angle and number of periodicity on dispersion and transmission curves, for linearly increasing and decreasing refractive index function on the longitudinal direction with and without defect layer of constant refractive index.

The aim of this work is to study the properties of the defect modes, the transmitted phase and intensity of a normally incident plane wave beam on a defective 1DPC structure with a r-GRIN defect layer. We have used the transfer matrix method to calculate the numerical evolution of the transmitted phase and intensity. Three r-GRIN distribution functions are applied to defect layer in the structure of  $(AB)^4C(AB)^4$ , where  $A$  and  $B$  are constant refractive index materials and  $C$  stands for r-GRIN defect layer. For these purposes, in Section 2, we have introduced the proposed PC structure and materials that are used. A short brief results of the transfer matrix calculation are also presented. The applied r-GRIN distribution functions are introduced and illustrated graphically. The behaviours of corresponding defect modes in the first band gap, the phase and intensity of the transmitted beam are presented in Section 3. Finally, the conclusions of the paper are summarized in the Section 4.

## 2. MODEL AND THEORY

Consider a binary defective 1DPC structure with arrangement of  $(AB)^4C(AB)^4$ , as schematically depicted in Fig. 1, where  $A$  and  $B$  are two kinds of different materials with constant refractive indexes of  $n_A = 1.38$  and  $n_B = 2.6$ , respectively.  $C$  stands for the r-GRIN defect layer, which is assumed a symmetric function of  $x$  and  $y$ , and homogenous in the  $z$  direction. So, it is better to use the cylindrical coordinate of  $r$  and  $z$ . All layers are placed on the  $x$ - $y$  plane. Three r-GRIN distribution functions of  $n_C = n_0(1 + a \exp(-(\frac{r}{r_0})^2))$ ,  $n_C = n_0(1 + a \cos^2(\pi \frac{r}{r_0}))$  and  $n_C = n_0(1 + a \sin^2(\pi \frac{r}{r_0}))$  are used, where  $r$  is the radial coordinate,  $n_0$  is the background refractive index and  $a$  is a parameter.  $a$  displays the amount of the defect layer refractive index gradient by an external parameter such as intensity or voltage. In numerical analysis,  $n_C$  and  $r$  are normalized to  $n_0$  and  $r_0$ , respectively. Fig. 2 depicts the profiles of the normalized refractive index distribution functions proposed for the defect layers. Thanks to the modern technological advantages, realization of such distribution functions inside a material is possible. Using the modulated electrical field [21], glancing angle deposition technique [22], optical holography and interferometric methods [23] are some of them. For the cases of under study, the intensity distributions of the Gaussian, the square of the sinc and cosine, can be produced by applying an intensity distribution of the Gaussian, which is the laser radiation fundamental mode, the performance of the diffraction pattern by a single slit or double-slit interference inside a photosensitive media, respectively. Then the refractive index of the medium will also be modulated accordingly.

In order to see the behaviour of the ray path inside the introduced r-GRIN defect layers, commonly

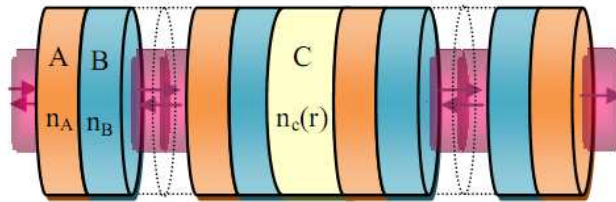


**Figure 1.** Schematic of a binary defective 1DPC structure, where layers  $A$  and  $B$  represent the constant refractive index materials with  $n_A = 1.38$  and  $n_B = 2.6$ , respectively and  $C$  stands for a r-GRIN defect layer.

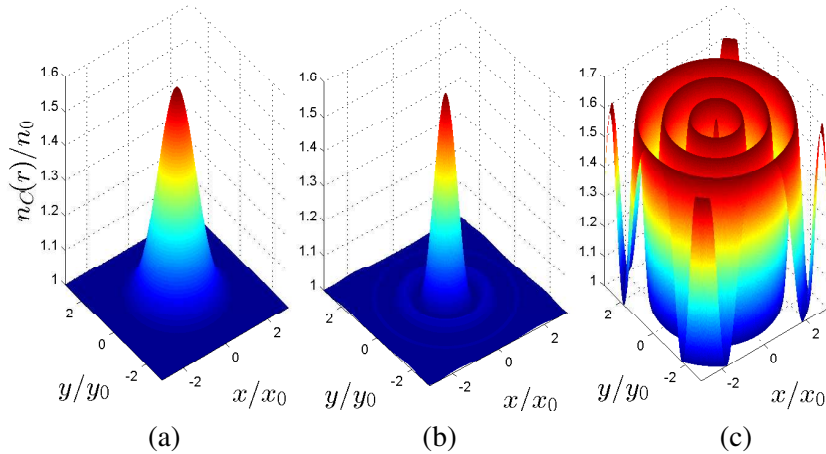


**Figure 2.** Profiles of the normalized refractive indices distribution functions of the (a) Gaussian, (b) square of the sinc and (c) square of the cosine r-GRIN proposed for the defect layer.

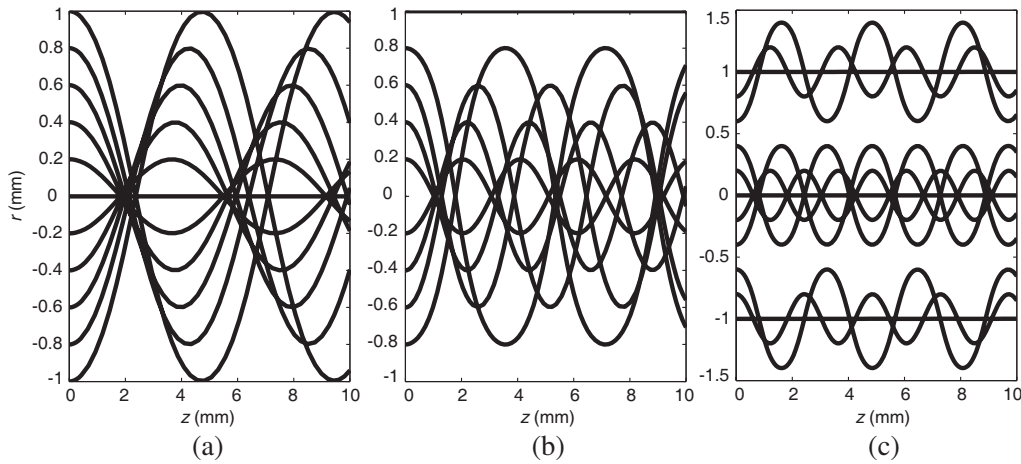


**Figure 3.** The behaviour of the ray path inside of the (a) Gaussian, (b) square of the sinc and (c) square of the cosine r-GRIN defect layers.

used vector form of the ray equation is solved numerically [24]:

$$\frac{d}{ds} \left( n(r) \frac{dr}{ds} \right) = \nabla n(r) \tag{1}$$

By considering these materials long, the ray paths are plotted in Fig. 3. Due to the inhomogeneity of the defect layer, the normally incident rays at the entrance surface will not be normal to the output surface and depend on  $r$ -coordinate. Therefore it is important to know the exit rays angle at the back surface of the defect layer. It will be necessary to calculate the transfer matrix form of the next layers correctly. In Fig. 4, we have plotted the behaviour of the rays angle in defect layer’s back surface versus the incident beam’s radial distance in its front surface for used nanoscale thicknesses. As it is seen obviously, the incident angles in the back surface of the defect layer are not considerable. Therefore, these small angles do not clearly influence our results in comparison with the normal incidents. Let a plane wave be normally incident from the vacuum into the PC structure (depicted in Fig. 1) propagating in the  $z$  direction. Different analytical and numerical methods are proposed to investigate the optical transmission of the PC structures [25–28]. Among them, the wave transfer matrix method is one of the simplest and most common methods to investigate the band gap characteristics of the transmittance spectrum and dispersion curves of the 1DPC [25].

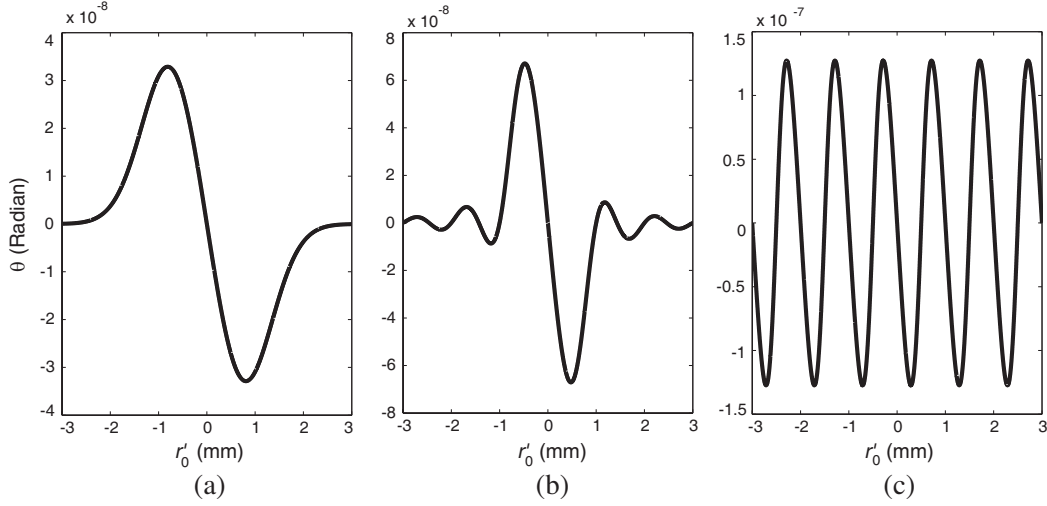


**Figure 4.** The behaviour of the rays angle  $\theta$  in defect layer's back surface versus the incident beam's radial distance  $r'_0$  in its front surface for the (a) Gaussian, (b) square of the sinc and (c) square of the cosine r-GRIN defect layers.

During the propagation of electromagnetic wave in the periodic layered structure, the electric vector  $E$  and the magnetic vector  $H$ , between one layer and its neighbor, are related by the following matrix:

$$M_j(\omega) = \begin{bmatrix} \cos k_j d_j & \frac{i}{n_j} \sin k_j d_j \\ i n_j \sin k_j d_j & \cos k_j d_j \end{bmatrix} \quad (2)$$

where  $i = \sqrt{-1}$ ,  $k_j = \frac{n_j \omega}{c}$ ,  $c$  is the speed of light in the vacuum, and  $d_j$  is the thickness of layers in which  $j = A, B, C$ . The transfer matrix of the whole structure is as following:

$$M(r, \omega) = [M_A(\omega)M_B(\omega)]^4 M_C(r, \omega) [M_A(\omega)M_B(\omega)]^4 = \begin{bmatrix} m_{11}(r, \omega) & m_{12}(r, \omega) \\ m_{21}(r, \omega) & m_{22}(r, \omega) \end{bmatrix} \quad (3)$$

The transmission coefficient in free space can be obtained from the total characteristic matrix elements as:

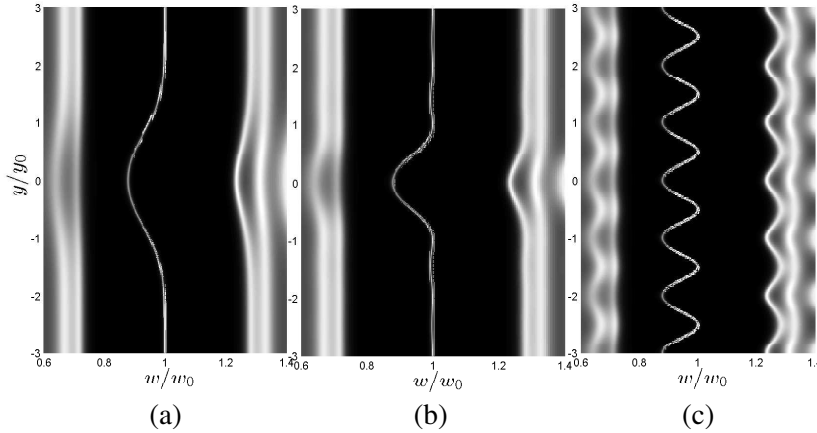
$$t(r, \omega) = \frac{2}{[m_{22}(r, \omega) + m_{11}(r, \omega)] - [m_{12}(r, \omega) + m_{21}(r, \omega)]} \quad (4)$$

The real and imaginary parts of  $t(r, \omega)$  give the amplitude and phase of the transmitted wave. The transmittance is given by  $T(r, \omega) = |t(r, \omega)|^2$ .

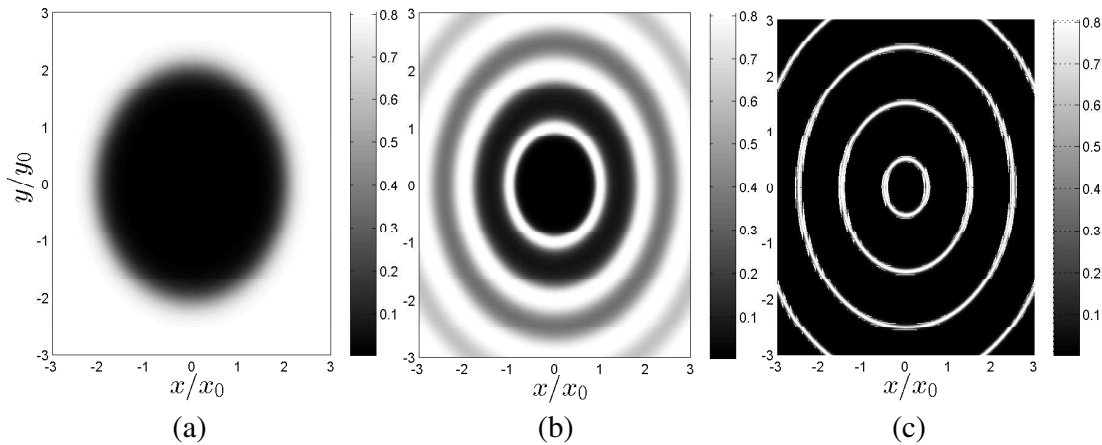
### 3. NUMERICAL RESULTS AND DISCUSSIONS

The material of the layer  $A$  is Magnesium fluoride ( $MgF_2$ ) with  $n_A = 1.38$  and the layer  $B$  is Zinc selenid ( $ZnSe$ ) with  $n_B = 2.6$ . The quarter-wave condition:  $n_A d_A = n_B d_B = n_C d_C = \lambda_0/4$  is applied for their thickness, where  $\lambda_0$  is the design wavelength and it is usually designed to fall around the center of optical spectrum ( $= 550$  nm). The parameter  $a$  is assumed to be 0.6.

Figure 5 shows the behaviour of the defect modes versus normalized frequency and transverse coordinate (for simplicity only direction of  $y$  is used). Three different r-GRIN defect layers inserted in the structure of  $(AB)^4C(AB)^4$ . Correspondingly, in Fig. 5 laterally varying defect modes with (a) distribution of the Gaussian, (b) the square of the sinc and (c) cosine functions are appeared. The behaviour of the defect modes can be used to design plane wave modulators from the proposed PC structures. As it is seen, the rays passing from the different lateral positions are localized on different frequencies. For example, in Fig. 5(a), for  $y = 0$ , the transmitted field is localized on  $\omega = 0.9\omega_0$ . On the other hand, for  $y = \pm 2y_0$  it is localized on  $\omega = \omega_0$  and for other positions this localization can happen on different frequencies with the trend of the Gaussian distribution. In two other ones Figs. 5(b) and (c), a same procedure is achievable but with the trends of the square of the sinc and cosine, respectively.



**Figure 5.** The behaviour of the resonant modes at the transmittance spectrum of the 1DPC structures with three proposed r-GRIN defect layers under the irradiation of the plane wave beam versus the frequency of incident wave and the normalized distance in the first band gap for the (a) Gaussian, (b) square of the sinc and (c) square of the cosine r-GRIN defect layers (top view). The dark region in the middle is the band gap and the white curve in it is the defect frequencies.



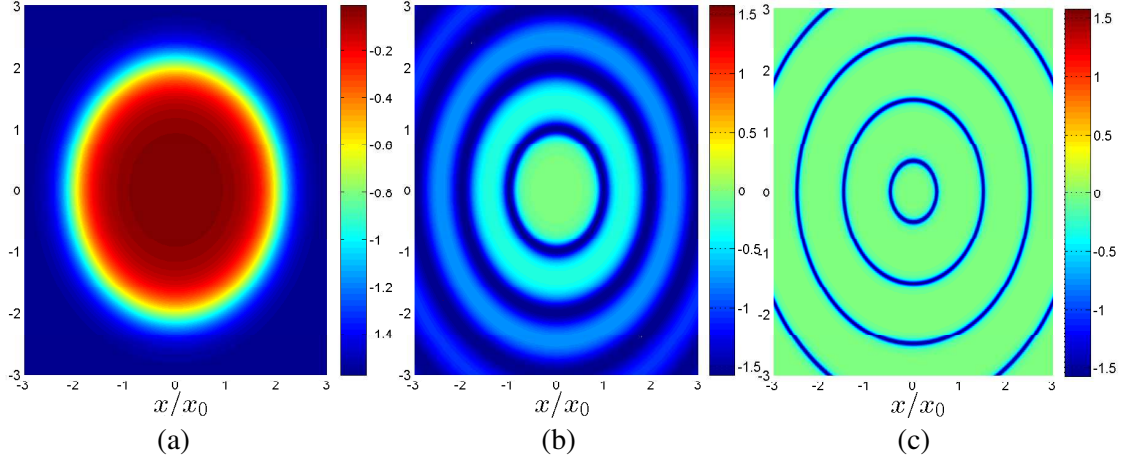
**Figure 6.** Transmission on the output plane versus the normalized  $y/y_0$  and  $x/x_0$  directions for incident frequency tuned to be  $\omega = \omega_0$  for the (a) Gaussian, (b) square of the sinc and (c) square of the cosine r-GRIN defect layers.

Figure 6 shows the transmission for  $\omega = \omega_0$  versus normalized  $y/y_0$  and  $x/x_0$ . It is obvious from the figure that it is possible to modulate the transmission by choosing different incident frequencies according to its usages.

In Fig. 7, the behaviour of the transmitted phases for three r-GRIN distribution functions is illustrated. The frequency of the incident field is set to be the band gap central frequency:  $\omega = \omega_0$ . It is clear in this figure that phases on the output plane of these photonic crystals are different from each other. So, these structures have the capability to modulate the phase of the plane wave on the output surface.

In Fig. 8, we have plotted the intensity of the transmitted field, on the exit surface of the PC structure ( $x$ - $y$  plane) for incident frequency of  $\omega = \omega_0$ . A single ring-shape intensity distribution is seen for the r-GRIN Gaussian function in Fig. 8(a). For the square of the sinc function Fig. 8(b), a corresponding intensity distribution is appeared and for the last r-GRIN function a periodic equal-spaced double ring intensity distribution is obtained. Possibility to make some changes in the plane wave's intensity distribution can be clearly seen in this figure.

In order to have an explicit understanding of the introduced plane wave modulators, it is useful to



**Figure 7.** The phase of the output wave on the output plane versus the normalized  $y/y_0$  and  $x/x_0$  directions for the incident frequency tuned to the center of the first band gap corresponding to the (a) Gaussian, (b) square of the sinc and (c) square of the cosine r-GRIN defect layers in PC.

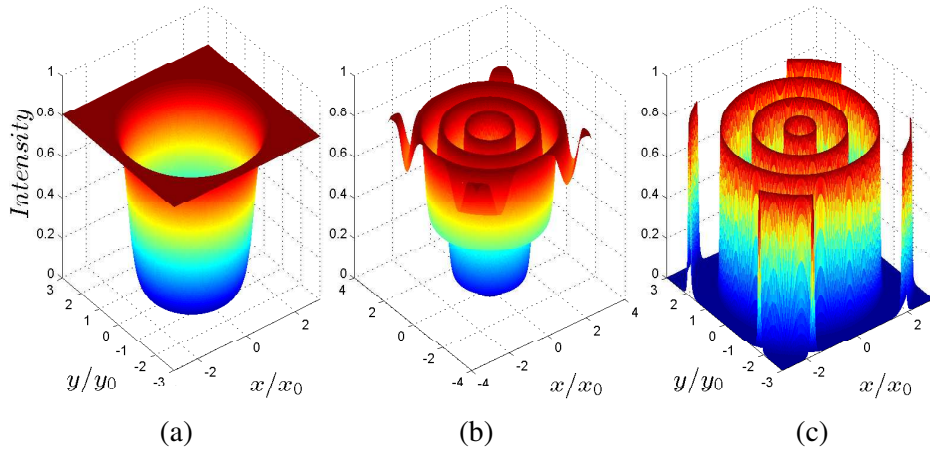


**Figure 8.** Intensity on the output plane versus the normalized directions at the center of the first band gap corresponding to the (a) Gaussian, (b) square of the sinc and (c) square of the cosine r-GRIN defect layers in PC.

compare the output intensities of different incident frequencies for 1DPC structures. Figs. 9, 10 and 11 show the output intensity for two incident frequencies of  $\omega = \omega_0$  and  $\omega = 0.99\omega_0$ .

It is obvious in these figures that choosing different incident frequencies and refractive index distribution functions for the defect mode can make some considerable changes in the output intensity. So, some desired plane wave modulators can be obtained by designing 1DPC structures using the proposed defect layers.

By considering the origin of the regular defect mode with a constant optical defect layer, the physical interpretation of these behaviours is very simple. While all applied light sources have a finite lateral extension, different rays can experience different optical paths. When such rays are passing through a r-GRIN layer, inserted on a PC structure, every traveling ray will cause different Bragg condition and corresponding defect mode will appear in PBG. Consequently, a localized defect mode according to the defect layer radial refractive index distribution function will appear. So, the phase and amplitude of an incident plane wave will be modulated on the output surface of the PC. In other words, on the output surface of the PC we will have a light surface that is distributed according to the defect layer refractive index distribution function. The propagation of these beams will cause different diffraction patterns at the far field (Fraunhofer diffraction).

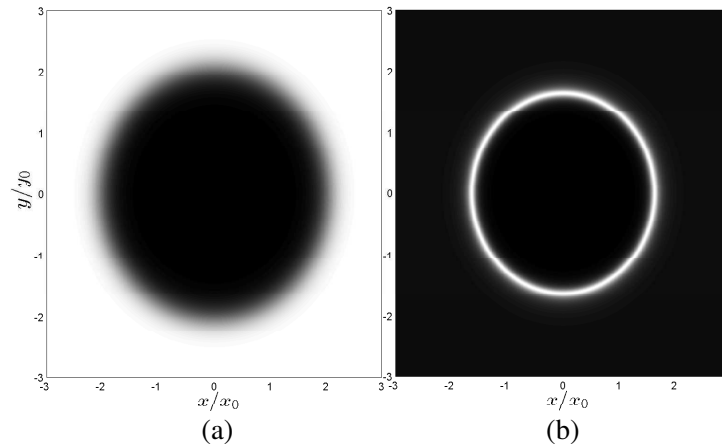


**Figure 9.** Intensity on the output plane versus the normalized directions for two frequencies of (a)  $\omega = \omega_0$  and (b)  $\omega = 0.99\omega_0$  for the Gaussian r-GRIN defect layer in PC.

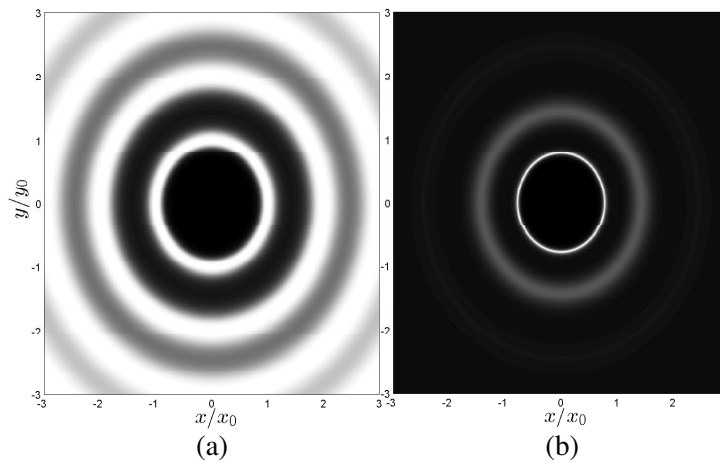


**Figure 10.** Intensity on the output plane versus the normalized directions for two frequencies of (a)  $\omega = \omega_0$  and (b)  $\omega = 0.99\omega_0$  for the square of the sinc r-GRIN defect layer in PC.

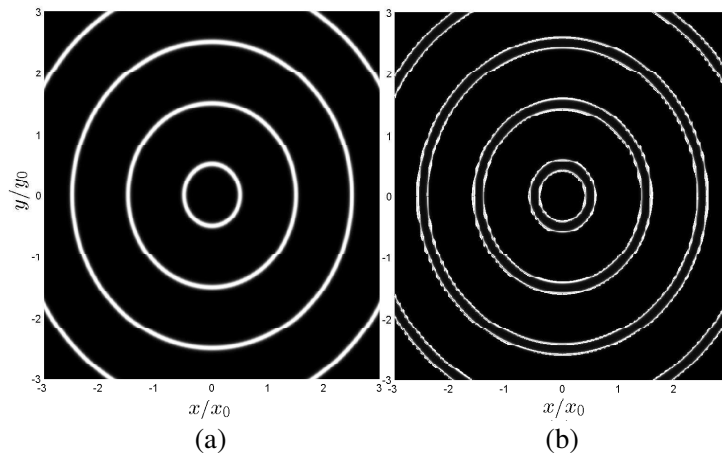


**Figure 11.** Intensity on the output plane versus the normalized directions for two frequencies of (a)  $\omega = \omega_0$  and (b)  $\omega = 0.99\omega_0$  for the square of the cosine r-GRIN defect layer in PC.

#### 4. CONCLUSION

We studied 1DPC structure with arrangement of  $(AB)^4C(BA)^4$ , that  $A$  and  $B$  represent the constant refractive index materials and  $C$  stands for a r-GRIN layer. In numerical analysis  $MgF_2$  ( $n_A = 1.38$ ),  $ZnSe$  ( $n_B = 2.6$ ) and quarter wavelength condition with design wavelength of  $\lambda = 550$  nm are applied for the layers  $A$ ,  $B$  and their thickness, respectively. The Gaussian, the square of the sinc and cosine distribution functions, which practically are utilizable, are proposed for the r-GRIN defect layer  $C$ . The behaviour of the defect modes spectrum with lateral coordinate, the phase and intensity of transmitting field, for different frequencies on the output surface of the structure ( $x$ - $y$  plane) are investigated. Radially varying defect modes, corresponding to the applied r-GRIN distribution function, appeared inside the band gap.

This study introduces the capability of the artificial PC structure to modulate the phase and amplitude of a plane wave, and make it possible to design required plane wave modulators. The results showed that the output intensity and phase closely depend on the defect layers refractive index distribution function and incident beams frequency. So, it is possible to change these factors to achieve some desired outputs.

#### REFERENCES

1. Rayleigh, J. W. S., "On waves propagating along the plane surface of an elastic solid," *Proc. London Math. Soc.*, Vol. 17, No. 1, 4–11, 1885.
2. Yablonovitch, E. and T. J. Gmitter, "Photonic band-gap structure: The face centered-cubic case employing nonspherical atoms," *Phys. Rev. Lett.*, Vol. 67, No. 17, 2295–2298, 1991.
3. John, S., "Strong localization of photons in certain disordered dielectric superlattices," *Phys. Rev. Lett.*, Vol. 58, No. 20, 2486, 1987.
4. Srivastava, R., K. B. Thapa, S. Pati, and S. P. Ojha, "Omni-direction reflection in one dimensional photonic crystal," *Progress In Electromagnetics Research B*, Vol. 7, 133–143, 2008.
5. Awasthi, S. K., U. Malaviya, S. P. Ojha, N. K. Mishra, and B. Singh, "Design of a tunable polarizer using a one-dimensional nanosized photonic band-gap structure," *Progress In Electromagnetics Research B*, Vol. 5, 133–152, 2008.
6. Banerjee, A., "Enhanced temperature sensing by using one-dimensional ternary photonic band gap structures," *Progress In Electromagnetics Research Letters*, Vol. 11, 129–137, 2009.
7. Wu, C. J., B. H. Chu, M. T. Weng, and H. L. Lee, "Enhancement of bandwidth in a chirped quarter-wave dielectric mirror," *Journal of Electromagnetic Waves and Applications*, Vol. 23, No. 4, 437–447, 2009.
8. Wu, C. J., B. H. Chu, and M. T. Weng, "Analysis of optical reflection in a chirped distributed Bragg reflector," *Journal of Electromagnetics Waves and Applications*, Vol. 23, No. 1, 129–138, 2009.
9. Wu, C. J., C. L. Liu, and W. K. Kuo, "Analysis of thickness-dependent optical properties in a one-dimensional superconducting photonic crystal," *Journal of Electromagnetic Waves and Applications*, Vol. 23, Nos. 8–9, 1113–1122, 2009.
10. Lotfi, E., K. Jamshidi-Ghaleh, F. Moslemi, and H. Masalehdan, "Comparison of photonic crystal narrow filters with metamaterials and dielectric," *Eur. Phys. J. D.*, Vol. 60, No. 2, 369–372, 2010.
11. Wu, C. J., J. J. Liao, and T. W. Chang, "Tunable multilayer Fabry-Perot resonator using electro-optical defect layer," *Journal of Electromagnetic Waves and Applications*, Vol. 24, No. 4, 531–542, 2010.
12. Wu, C. J. and Z. H. Wang, "Properties of defect modes in one-dimensional photonic crystals," *Progress In Electromagnetics Research*, Vol. 103, No. 10, 169–184, 2010.
13. Li, X., K. Xie, and H. M. Jiang, "Properties of defect modes in one-dimensional photonic crystals containing two nonlinear defects," *Opt. Commun.*, Vol. 282, No. 21, 4292–4295, 2009.
14. Martinez-Sala, R., J. Sancho, J. V. Sanchez, V. Gomez, and J. Llinares, "Sound attenuation by sculptures," *Nature*, Vol. 378, 241, 1995.

15. Torrent, D., A. Hakansson, F. Cervera, and J. Snchez-Dehesa, "Homogenization of 2D clusters of rigid rods in air," *Phys. Rev. Lett.*, Vol. 96, No. 20, 204302, 2006.
16. Jamshidi-Ghaleh, K. and Z. Safari, "Effect of a subwavelength layer on all optical-diode action in 1D photonic crystal," *Int. J. Mod. Phys. Conf. Ser.*, Vol. 15, 48–53, 2012.
17. Lotfi, E., K. Jamshidi-Ghaleh, F. Moslemi, and H. Masalehdan, "Optical multistability in 1D photonic crystals with nonlinear ThueMorse structure," *App. Phy. A*, Vol. 103, No. 3, 669–672, 2011.
18. Abdi-ghaleh, R., K. Jamshidi-Ghaleh, A. Namdar, and T. Touhidi, "Ring shape output intensity profile of a 1D photonic crystal micro-cavity irradiated by a gaussian beam," *Journal of Electromagnetic Waves and Applications*, Vol. 25, Nos. 5–6, 733–742, 2011.
19. Wu, X. Y., B. Zhang, J. Yang, X. Liu, N. Ba, Y. Wu, and Q. Wang, "Function photonic crystals," *Physica E*, Vol. 43, No. 9, 1694–1700, 2011.
20. Wu, X. Y., B. Zhang, J. Yang, S. Zhang, X. Liu, J. Wang, N. Ba, Z. Hua, and X. Yin, "The characteristic of light transmission of function photonic crystals," *Physica E*, Vol. 44, No. 7, 1223–1229, 2012.
21. Smith, T. W. and G. E. Wnek, "Modulation of refractive index in polymer composites: Toward a synthetic bio-optic lens," *Proc. SPIE — Int. Soc. Opt. Eng.*, Vol. 5051, 389–399, 2003.
22. Van Popta, A. C., M. M. Hawkeye, J. C. Sit, and M. J. Brett, "Gradient-index narrow-bandpass filter fabricated with glancing-angle deposition," *Opt. Lett.*, Vol. 29, No. 21, 2545–2547, 2004.
23. Kharitonov, M., N. Shatokhina, T. Sultanov, V. Zubov, and W. Staude, "Application of speckle interferometry to the analysis of refractive-index gradients in flows," *JRLR*, Vol. 20, No. 2, 171–178, 1999.
24. Born, M. and E. Wolf, *Principles of Optics*, Pergamon Press, Oxford, 1980.
25. Yariv, A. and P. Yeh, *Optical Waves in Crystals*, Wiley-Interscience, New York, 1989.
26. Pendry, B., "Photonic band structures," *J. Mod. Opt.*, Vol. 41, No. 2, 209–229, 1994.
27. Li, Z. Y., J. Wang, and B. Y. Gu, "Creation of partial band gaps in anisotropic photonic-band-gap structures," *Phys. Rev. B*, Vol. 58, No. 7, 3721, 1998.
28. Taflove, A., *Computational Electrodynamics*, Artech House INC, Norwood, 2000.